Real-time State of Charge Estimation of Electrochemical Model for Lithium-ion Battery

Chuanxin Fan
WMG
University of Warwick
Coventry, United Kingdom
Chuanxin.fan@warwick.ac.uk

Matthew D. Higgins
WMG
University of Warwick
Coventry, United Kingdom
M.Higgins@warwick.ac.uk

Widanalage D. Widanage
WMG
University of Warwick
Coventry, United Kingdom
Dhammika.widanalage@warwick.ac.uk

***Abstract*—This paper proposes the real-time Kalman filter based observer for Lithium-ion concentration estimation for the electrochemical battery model. Since the computation limitation of real-time battery management system (BMS) micro-processor, the battery model which is utilized in observer has been further simplified. In this paper, the Kalman filter based observer is applied on a reduced order model of single particle model to reduce computational burden for real-time applications. Both solid phase surface lithium concentration and battery state of charge (SoC) can be estimated with real-time capability. Software simulation results and the availability comparison of observers in different Hardware-in-the-loop simulation setups demonstrate the performance of the proposed method in state estimation and real-time application.**

Keywords— Battery Model, Battery Management Systems, Hardware-in-the-loop Simulation, State of Charge Estimation

I. INTRODUCTION

Nowadays, due to the climate warming and environmental degradation, the global automotive industry has been significantly accelerating the vehicle electrification process. Therefore, there is a growth in electric vehicles (EVs) designed and manufactured by many major automotive manufacturers. Due to the excellent performance of energy density and safety concern, the lithium-ion battery has been commonly utilized in EVs as energy storage system [1]. In general, only a lithium-ion battery's output current, voltage and surface temperature can be measured in an actual EV battery management system. Hence, in order to monitor the complex electrochemical dynamic processes inside batteries and estimate unmeasurable variables for practical application, advanced battery models and state estimation methods in battery management system (BMS) are imperative for the Electric Vehicles industry. Newman and his colleagues developed pseudo-two-dimension (P2D) model which is widely applied in academic research in 1993. The P2D model relies on five key partial differential equations to express kinetics (electrochemical), transport, and thermodynamic processes along with the geometry of the lithium-ion battery system [2][3]. However, the P2D model still faces obstacles to be utilized in the real-time industrial applications. Because of the computational limitation of BMS microprocessors, the relevant models which are used in the BMS should be appropriately simplified to satisfy the real-time application. In electric vehicles, the higher resolution is extremely vital for real-time application, since lots of instantaneous acceleration and braking dynamics take place within a very short time. Moreover, for safety concerns, the timely response is necessary for the BMS to protect drivers and vehicles as well. For example, in the case of dSPACE hardware-in-the-loop (HIL) simulation platform which is widely applied in real-world automotive industrial testing, each iterative operation step must be strictly computed within the specific simulation period. If the system model is too complicated or contains too many computations, the dSPACE device will overrun and fail consequently.

In order to be used for real-time and control-oriented application, the P2D model has been further simplified by assuming the solid-phase Li concentration in each electrode is constant in spatial coordinate, uniformly in time, named single particle model (SPM) [4][5][6][7]. And then, several state estimators/observers were designed based on the SPM to estimate the state-of-charge (SoC) for further vehicle's energy management strategy [4][7][8]. For instance, the simplified electrochemical model, e.g. Single Particle Model with electrolyte (SPMe), has been proposed by Moura et al [7]. In addition, the relevant PDE observer, named backstepping observer, has been also applied on SPMe in the same literature.

However, the abovementioned models haven't been applied in a real-time hardware-in-the-loop simulation platform yet. On the other hand, some tests showed that, even though the computational burden has been reduced by SPM and the corresponding observer, for high resolution in real-time hardware-in-the-loop simulation, these models are still too complicated to be processed by actual microprocessor. In this paper, the SPMe was further simplified by order reduction method to the Reduced Order Model with Nonlinear (ROM-NL), the Kalman filter was designed for this reduced concentration dynamic subsystem as the optimal observer for solid phase surface lithium concentration and SoC estimation. In addition, the proposed models were applied in a dSPACE device for real-time HIL simulation.

In Section 2, the single particle model with electrolyte and reduced order model of Li-ion battery in this paper are discussed. General overview of the proposed state estimation method is presented with equations and block diagrams in Section 3. Furthermore, the principles of output function inversion and Kalman filter are reviewed in Section 3 as well. Conducted simulation tests can be found in Section 4 together with discussion on the results, while the conclusion and future work on paper are given in Section 5.

II. BATTERY MODELS

In this paper, the single particle model with electrolyte (SPMe) has been utilized as battery plant cell, and the Reduced Order Model with Nonlinear (ROM-NL) was the model in the Kalman filter based observer for concentration dynamic subsystem estimation.

A. Single Particle Model with Electrolyte (SPMe)

To reduce the model complexity, Moura et al [7] proposed the SPMe model after introducing a few simplifications to the

P2D model. Each electrode is idealized as a single spherical particle, and the molar ion flux j is assumed constant in the x-direction in Fig. 1. This leads to a linear relationship between j and the input current I as follows (1),

$$j_n^-(t) = \frac{I(t)}{Fa^-L^-},\ j_n^+(t) = -\frac{I(t)}{Fa^+L^+} \tag{1}$$

Note that here positive current stands for discharging, and negative current for charging.

Then the PDEs in the P2D model become decoupled, as shown in Fig. 1. The dynamics of lithium concentration in the solid and electrolyte phases in Fig. 1 are given below. Note that $\{+, sep, -\}$ stand for the positive electrode (PE), separator, and negative electrode (NE) domain, respectively [7].

The evolution of lithium concentration in the solid phase follows (2),

$$\frac{\partial c_s^\pm}{\partial t}(r,t) = \frac{1}{r^2}\frac{\partial}{\partial r}\left[D_s^\pm r^2 \frac{\partial c_s^\pm}{\partial r}(r,t)\right] \tag{2}$$

with boundary conditions in (3),

$$\frac{\partial c_s^\pm}{\partial r}(0,t) = 0,\ \frac{\partial c_s^\pm}{\partial r}(R_s^\pm,t) = \pm\frac{1}{D_s^\pm Fa^\pm L^\pm} I(t) \tag{3}$$

The evolution of lithium concentration in the electrolyte phase follows (4)(5)(6),

$$\varepsilon_e^- \frac{\partial c_e^-}{\partial t}(x,t) = \frac{\partial}{\partial x}\left[D_e^{eff}(c_e^-)\frac{\partial c_e^-}{\partial x}(x,t)\right] + \frac{1-t_c^0}{FL^-} I(t) \tag{4}$$

$$\varepsilon_e^{sep} \frac{\partial c_e^{sep}}{\partial t}(x,t) = \frac{\partial}{\partial x}\left[D_e^{eff}(c_e^{sep})\frac{\partial c_e^{seo}}{\partial x}(x,t)\right] \tag{5}$$

$$\varepsilon_e^+ \frac{\partial c_e^+}{\partial t}(x,t) = \frac{\partial}{\partial x}\left[D_e^{eff}(c_e^+)\frac{\partial c_e^+}{\partial x}(x,t)\right] - \frac{1-t_c^0}{FL^+} I(t) \tag{6}$$

with boundary conditions in (7),

$$\begin{aligned}
&\frac{\partial c_e^j}{\partial x}(0^-,t) = \frac{\partial c_e^j}{\partial x}(0^+,t) = 0 \\
&D_e^{-,eff}(c_e(L^-))\frac{\partial c_e^-}{\partial x}(L^-,t) = D_e^{sep,eff}(c_e(0^{sep}))\frac{\partial c_e^{sep}}{\partial x}(0^{sep},t) \\
&D_e^{+,eff}(c_e(L^+))\frac{\partial c_e^+}{\partial x}(L^+,t) = D_e^{sep,eff}(c_e(L^{sep}))\frac{\partial c_e^{sep}}{\partial x}(L^{sep},t) \\
&c_e(L^-,t) = c_e(0^{sep},t),\ c_e(L^+,t) = c_e(L^{sep},t)
\end{aligned} \tag{7}$$

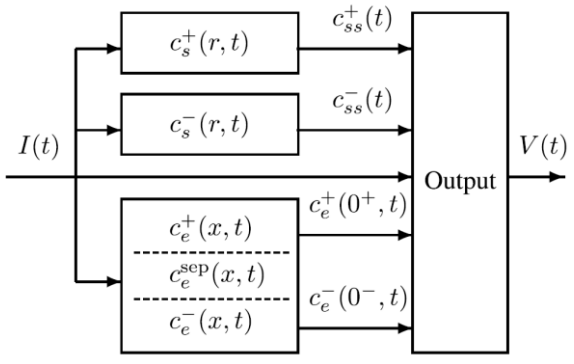

Fig.1. The block diagram of the SPMe [9]

Finally, the terminal voltage output is a nonlinear function of the PE and NE surface lithium concentrations ($c_{ss}^+(t)$ and $c_{ss}^-(t)$), the electrolyte lithium concentrations at the positive and negative current collectors ($c_e(0^+,t)$ and $c_e(0^-,t)$, respectively), and the input current $I(t)$, as in (8):

$$\begin{aligned}
V(t) &= U^+(c_{ss}^+(t)/c_{s,\max}^+) - U^-(c_{ss}^-(t)/c_{s,\max}^-) \\
&+ k_{conc}\left[\ln\left(c_e(0^+,t)\right) - \ln\left(c_e(0^-,t)\right)\right] \\
&+ \left[\frac{L^+ + 2L^{sep} + L^-}{2\bar{\kappa}} - \left(\frac{R_f^+}{a^+L^+} + \frac{R_f^-}{a^-L^-}\right)\right] I(t) \\
&+ \frac{RT}{\alpha F}\left[\sinh^{-1}\left(-\frac{I(t)}{2a^+L^+ i_0^+(t)}\right) - \sinh^{-1}\left(\frac{I(t)}{2a^-L^- i_0^-(t)}\right)\right]
\end{aligned} \tag{8}$$

where $i_0^\pm$ represents the exchange current density, and

$$i_0^\pm(t) = k^\pm\left[c_{ss}^\pm(t)\right]^{\alpha_c} \times \left[c_e(0^\pm,t)\left(c_{s,\max}^\pm - c_{ss}^\pm(t)\right)\right]^{\alpha_a} \tag{9}$$

The readers can refer to for [7] more details of the derivation of the SPMe equations.

B. SPMe numerical solution

To solve the SPMe equations, the same procedure in [7] is followed here. The evolution of lithium concentration in the electrode and electrolyte domains are solved separately.

1) Electrode concentration dynamics

The average lithium concentration in the electrode, or bulk concentration , is an integration of the current [9],

$$\frac{\overline{C_s^\pm}(s)}{I(s)} = \pm\frac{3}{R_s^\pm a^\pm FL^\pm}\frac{1}{s} \tag{10}$$

where the $\overline{C_s^\pm}(s)$ is the Laplace transformation of $\overline{c_s^\pm}(t)$, and $I(s)$ is the Laplace transformation of the current. Similar notations will apply hereinafter.

Define the difference between the electrode surface concentration and bulk concentration as $\Delta c_s^\pm(t) = c_{ss}^\pm(t) - \overline{c_s^\pm}(t)$. Then according to the transcendental transfer function proposed in,

$$\frac{\Delta C_s^\pm(s)}{I(s)} = \frac{R_s^\pm}{D_s^\pm}\frac{\left[(\beta^\pm)^2+3\right]\tanh(\beta^\pm) - 3\beta^\pm}{(\beta^\pm)^2\left[\tanh(\beta^\pm) - \beta^\pm\right]} \tag{11}$$

where $\beta^\pm = R_s^\pm\sqrt{s/D_s^\pm}$. Equation (11) can be reformulated into the partial fraction expansion, neglecting the high frequency dynamics above a cut-off frequency (here 10 Hz),

$$\frac{\Delta C_s^\pm(s)}{I(s)} \approx Z_s^\pm + \sum_{k=1}^{n_s^\pm}\frac{r_k^\pm s}{s - p_k^\pm} \tag{12}$$

The readers can refer to [9] for more details. Next, Equation (12) can be readily put into state-space form as

$$\begin{aligned}
\dot{x}_s^\pm(t) &= A_s^\pm x_s^\pm(t) + B_s^\pm I(t) \\
\Delta c_s^\pm(t) &= C_s^\pm x_s^\pm(t) + D_s^\pm I(t)
\end{aligned} \tag{13}$$

Where $x_s^\pm(t)$ is a vector representing the concentration $c_s^\pm(x,t)$ at the discrete nodes.

2) Electrolyte concentration dynamics

The electrolyte concentration dynamics in (4)(5)(6) is discretized by finite element method, yielding

$$\begin{aligned}\dot{x}_e(t) &= A_e x_e(t) + B_e I(t)\\ c_e(0^+,t) &= C_e^+ x_e(t), \quad c_e(0^-,t) = C_e^- x_e(t)\end{aligned} \tag{14}$$

where $x_e(t)$ is a vector representing the concentration $c_e(x,t)$ at the discrete nodes. Equation (14) can be further simplified by removing the pole/zero cancellation at the origin, as shown in [9].

C. Reduced Order Model with Nonlinear (ROM-NL)

As a comparison with the ECM, the ROM-NL is derived from the SPMe. The ideas here is to approximate the linear concentrations dynamics in (12) and (14) with low order models, while maintaining the nonlinear voltage output equation. Equation (12) and (14) are simplified to (15) and (16), respectively, using the balanced truncation method in [9]. Again, the truncated Hankel values should account for no more than 0.5% of the sum of all system Hankel values.

$$\begin{aligned}\dot{x}^{\pm}_{s,rom}(t) &= A^{\pm}_{s,rom} x^{\pm}_{s,rom}(t) + B^{\pm}_{s,rom} I(t)\\ c^{\pm}_{ss,rom}(t) &= C^{\pm}_{s,rom} x^{\pm}_{s,rom}(t) + D^{\pm}_{s,rom} I(t)\end{aligned} \tag{15}$$

$$\begin{aligned}\dot{x}_{e,rom}(t) &= A_{e,rom} x_{e,rom}(t) + B_{e,rom} I(t)\\ c_{e,rom}(0^+,t) &= C^{+}_{e,rom} x_{e,rom}(t) + D^{+}_{e,rom} I(t)\\ c_{e,rom}(0^-,t) &= C^{-}_{e,rom} x_{e,rom}(t) + D^{-}_{e,rom} I(t)\end{aligned} \tag{16}$$

The voltage output is calculated using the concentration outputs of the ROMs,

$$\begin{aligned}V(t) = {} & U^+(c^+_{ss,rom}(t)/c^+_{s,\max}) - U^-(c^-_{ss,rom}(t)/c^-_{s,\max})\\ & + k_{conc}\left[\ln\left(c_{e,rom}(0^+,t)\right) - \ln\left(c_{e,rom}(0^-,t)\right)\right]\\ & + \left[\frac{L^+ + 2L^{sep} + L^-}{2\bar{\kappa}} - \left(\frac{R^+_f}{a^+L^+} + \frac{R^-_f}{a^-L^-}\right)\right] I(t)\\ & + \frac{RT}{\alpha F}\left[\sinh^{-1}\left(-\frac{I(t)}{2a^+L^+ i^+_{0,rom}(t)}\right) - \sinh^{-1}\left(\frac{I(t)}{2a^-L^- i^-_{0,rom}(t)}\right)\right]\end{aligned} \tag{17}$$

where $i^{\pm}_{0,rom}(t) = k^{\pm}\left[c^{\pm}_{ss,rom}(t)\right]^{\alpha_c} \times \left[c_{e,rom}(0^{\pm},t)\left(c^{\pm}_{s,\max} - c^{\pm}_{ss,rom}(t)\right)\right]^{\alpha_a}$.

III. State Estimation Method

This paper expanded the strategy inspired by [7] to the further simplified observer for real-time application. In this study, Kalman filter which is applied on ROM-NL has been utilized as the basis of the proposed observer, such that it's able to achieve the goal of decreasing the amount of computation for real-time application.

A. Observer Design

This observer comprises two subsystems: Output Function inversion and the solid phase concentration Kalman Filter. In this paper, the observer schematic is shown in Fig. 2.

The observer process is listed as follow,

1) Once the voltage error is calculated from battery cell voltage $V(t)$ and observer estimated voltage $\hat{V}(t)$, the output function inversion can calculate the inversion cathode surface concentration $c^+_{ss}(t)$. Consequently, with the assumption conservation of mass, the inversion estimated anode surface concentration $c^-_{ss}(t)$ can be resulted.

2) With the inversion estimated concentrations and input current, the standard Kalman filters based on ROM-NL for both electrode concentration dynamic subsystems can be implemented. Next, the both electrodes estimated surface concentrations $c^{\pm}_{ss}(t)$ and bulk concentrations $\bar{c}^{\pm}_{s}(t)$ can be observed by each Kalman filter.

3) Finally, the estimated solid phase surface concentrations and electrolyte concentrations are fed into observer nonlinear output function subsystem which is same as the function in SPMe to produce the observer estimated output voltage $\hat{V}(t)$.

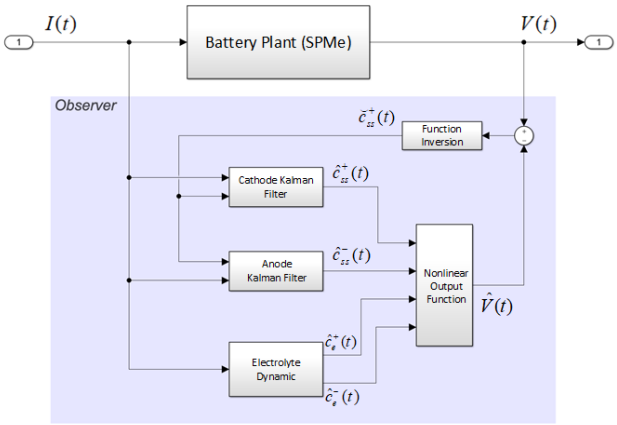

Fig.2. The Schematic of observer design

B. Output Function Inversion

This section is about a nonlinear gradient algorithm to calculate cathode concentration from measurements $I(t)$ and $V(t)$ by inverting the nonlinear output function of the SPMe. Note that this method assumes the output function only depends on cathode concentration and time t as

$$V(t) = g(c^{\pm}_{ss}(t), t) \tag{18}$$

The inversion result from output function can be represented as $\breve{c}^+_{ss}(t)$. And then, expand the output function by Taylor series with respect to the difference between $c^+_{ss}(t)$ and $\breve{c}^+_{ss}(t)$ about equals to zero. Finally, rewrite the nonlinear output function in 'Gradient Method' [10] form and the gradient update law for $\hat{c}^+_{ss}(t)$ to minimizes $\frac{1}{2}\lambda(g(c^+_{ss}(t),t) - g(\breve{c}^+_{ss}(t),t))^2$ is given by,

$$\frac{d}{dt}\breve{c}^+_{ss}(t) = \lambda \bullet (g(c^+_{ss}(t),t) - g(\breve{c}^+_{ss}(t),t)) \bullet \frac{\partial}{\partial c^+_{ss}(t)} g(\breve{c}^+_{ss}(t),t) \tag{19}$$

where the gain λ is to compromise between accuracy and speed.

C. Backstepping Observer

The backstepping observer is a Luenberger-type observer which can be applied on original partial differential equations (PDEs) directly before discretization and the physical

significance of the PDEs is still retained. Furthermore, this observer has been utilized in SPMe in [7] to estimate the distribution of solid phase lithium ion concentration. The readers can refer to [7] for more details.

D. Kalman Filter

Kalman filter utilizes a system's input and output data to seek for the optimal state of linear systems under process and measurement white noise. The discrete-time system can be represented as follow:

$$X_k = AX_{k-1} + BU_{k-1} + w_{k-1} \tag{20}$$

$$Y_k = CX_k + v_k \tag{21}$$

Where X represents the states of system, Y denotes the output of estimation, u is the model input and here is the current, A represents the state transition matrix, B denotes control-input matrix, C denotes measurement matrix, and index $k, k-1$ denote time steps of system, while w_k represents the system process noise and v_k represents measurement noise, respectively. These two variables are defined as white noise and with Gaussian probability distributions:

$$p(w_k) \sim N(0, Q) \tag{22}$$

$$p(V_k) \sim N(0, R) \tag{23}$$

Where Q and R represents process noise and measurement noise covariance matrices.

Then the estimation of the state vector $\hat{X}_k$ and output $\hat{Y}_k$ by Kalman filter algorithm could be mathematically expressed as 'Prediction Time Update' and 'Measurement Update'. In addition, the symbol '$^-$' means the priori variables in each time step.

Prediction Time Update:

$$\hat{X}_k = A\hat{X}_{k-1} + BU_{k-1} + w_{k-1} \tag{24}$$

$$P_k^- = A_k P_{k-1} A_k^T + Q_{k-1} \tag{25}$$

$$\hat{Y}_k = C\hat{X}_k^- + v_k \tag{26}$$

Measurement Update:

$$K_k = P_k^- C_k^T (C_k P_k^- C_k + R_{k-1}) \tag{27}$$

$$\hat{X}_k = \hat{X}_k^- + K_k (Y_k - \hat{Y}_k) \tag{28}$$

$$P_k = (I - K_k C_k) P_k^- \tag{29}$$

The Kalman filter can provide the optimal state estimations, and its error elimination ability is suitable for practical real-time application. The readers can refer to [11] for more details.

IV. Simulation Results

In this section, the simulation platform and initial conditions are presented. The battery model SPMe and Kalman filter based observer are implemented in 'MATLAB/Simulink 2017b', and then, these models are downloaded in the hardware device 'SCALEXIO' from 'dSPACE' for hardware-in-the-loop simulation in real-time application.

Since both the battery plant and observer are to start from equilibrium states, the solid phase surface concentration was equal to bulk concentration. Therefore, the initial conditions along the radius were same in battery plant each electrode. As for the observer, only two bulk concentration states need to be the initial condition, and the other states should be set as zero. In order to display the observer's ability of the error reduction, the initial conditions have been set as different values as Table I.

Table I. Initial Conditions of System Model Variable

	Electrodes Initial Concentration $(^{mol}/_{m^3})$	
	Positive Electrode	***Negative Electrode***
Battery Plant	3000	30000
Kalman Filter	3900	21000
Output Inversion	2700	/

Note that the total moles of lithium in the electrolyte in the battery and observer are known beforehand and might be provided by the manufacturer [7].

In this paper, the reference current profile of the simulations were the city drive cycle 'FTP-75' (EPA Federal Test Procedure), with capped current magnitude at 1.5C, as Fig. 3.

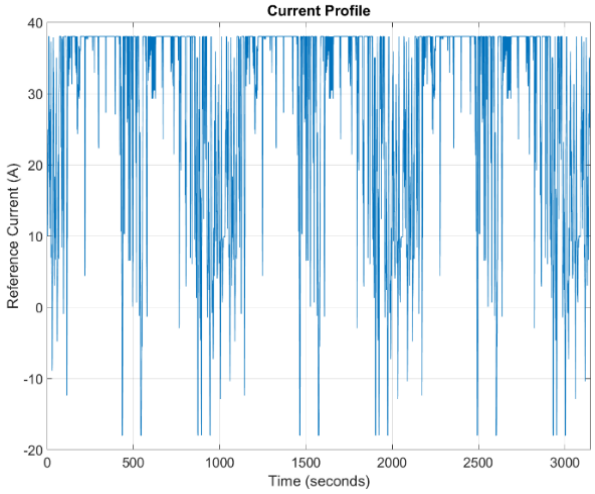

Fig.3. the FTP-75 Current Profile

A. Software Simulation results

From Fig. 4 and Fig. 5, the output voltage of the observer has been presented and compared with battery plant's voltage. Even the initial voltage output of the observer was different from battery plant, the observer can still closely converge to plant's output. The reason of the fluctuation in the end should be from the model reduction error and the anode surface concentration conversion process. But the voltage error is still acceptable with a maximum error of less than 10mV [1] for the real-time electric vehicle application.

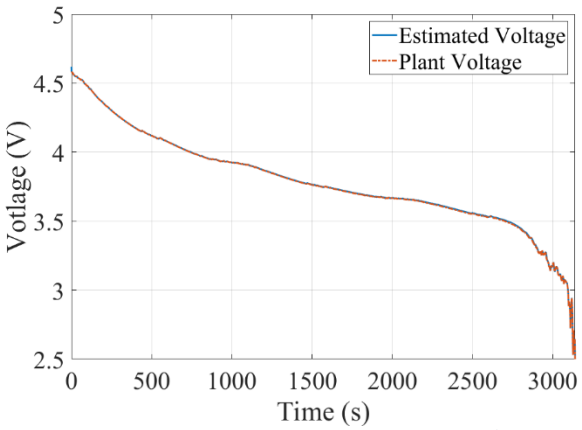

Fig.4. Battery Plant and Observer Voltage Profiles

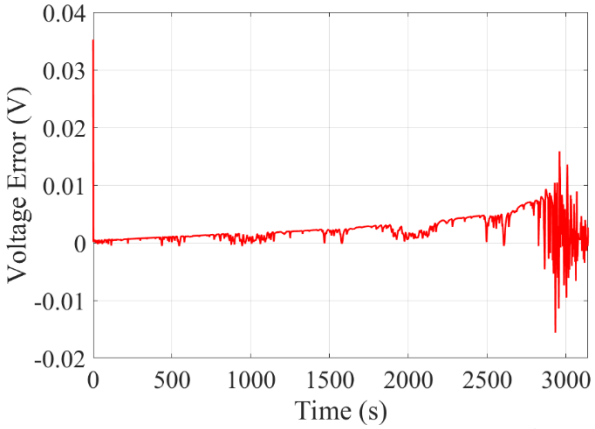

Fig.5. Battery Plant and Observer Voltage Error Profiles

The Fig. 6 and Fig. 7 show the performance of the observer estimated solid phase surface Lithium-ion concentration. Even though the initial conditions were set differently, the observer can promptly track to the actual surface concentration state and roughly fit the plant's concentration profile.

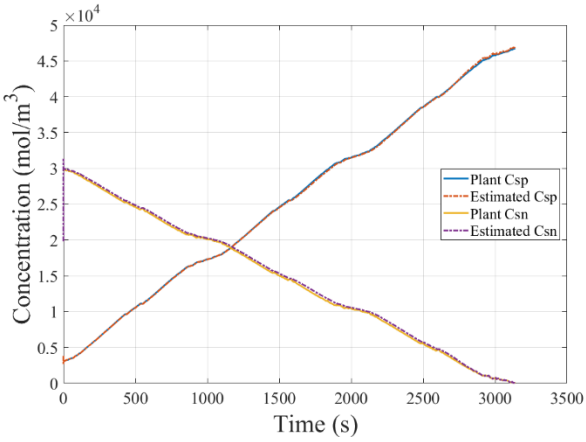

Fig.6. Battery Plant and Observer Surface Concentration Profiles

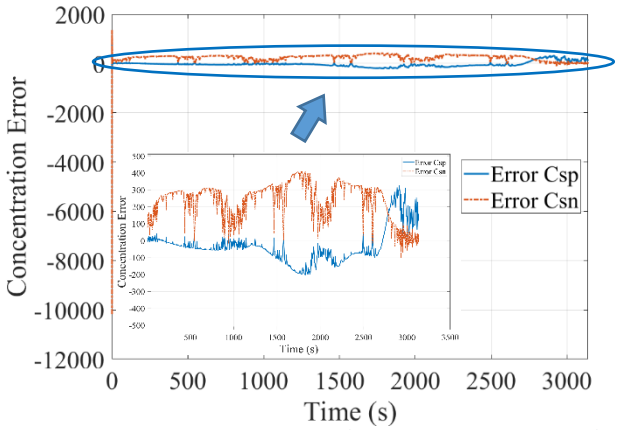

Fig.7. Battery Plant and Observer Surface Concentration Error Profiles

In Fig.7, the surface concentration mole errors between the plant and observer were indicated, and after the beginning of observer tracking process, the cathode error could retain less than 1% in the all discharge regime. Furthermore, in practice, in order to improve battery life, batteries should be designed not to discharge to ultimate state. Therefore, the proposed observer can be acceptable for the solid phase surface concentration estimation.

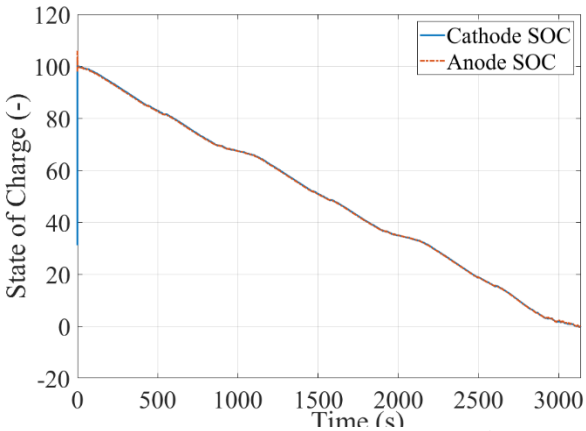

Fig.8. Battery Plant and Observer SOC Profiles

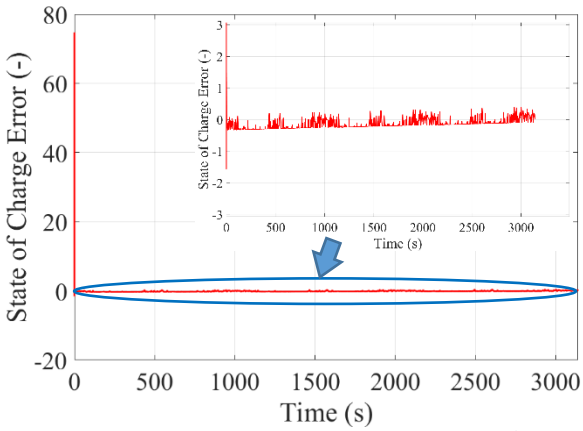

Fig.9. Battery Plant and Observer SOC Error Profile

Additionally, in Fig. 8 and Fig. 9, the other objective of the proposed observer SOC estimation in both electrodes is shown. Since in the ROM-NL, the electrode bulk lithium concentration state is designed. And the change of SOC is directly related to the change of Lithium ion bulk

concentration in the electrodes [8]. According to the bulk concentration, the SOC can be estimated for each electrode by following SOC definition equations:

$$SOC^{\pm} = \frac{\overline{C_s^{\pm}}(s) - C_{s,SOC=0\%}^{\pm}}{C_{s,SOC=100\%}^{\pm} - C_{s,SOC=0\%}^{\pm}} \tag{30}$$

After short tracking process, both electrodes SOC were almost overlapped in the whole operational process. And the SOC error between these two electrode observers were less than 0.5% as Fig. 9.

B. Hardware-in-the-loop Simulation Setup

In this paper, both the proposed Kalman filter based observer (KF) and the Backstepping observer (BO) in [7] have been implemented in hardware-in-the-loop simulation device 'SCALEXIO' from dSPACE Ltd. In the dSPACE platform, the Run-Time Behaviour 'Period' controls the period of a periodic task or the period constraint of a runnable function. On the other hand, in Simulink, the step size specifies the fundamental sample time used by the selected fixed-step solver. These two setups control the resolution performance of the proposed model in HIL simulation. Compared by the availability of two observers in different setups Run-Time Behaviour 'Period' (in SCALEXIO) and Step Size (in Simulink) as Table II, the proposed observer has higher resolution in the real-time platform application, the Kalman filter based observer is able to be utilized in a shorter sample period to provide as many as information data.

In the real-time electric vehicle applications, the BMS should have the higher resolution to promptly respond to emergencies and record batteries operating behaviours. With the same Simulink Step-size, the 0.1s period resolution of the Kalman filter based observer can be more suitable for most of practical applications in real-time.

Table II. Availability of KF and BO for Different HIL Platform Setups

Step Size \ HIL Platform 'Period'	***0.01s***	***0.1s***	***1s***
0.01s	None	KF	KF & BO
0.1s	None	KF	KF & BO
1s	None	KF	KF & BO

V. CONCLUSION

As the above results, the Reduced Order Model with Nonlinear (ROM-NL) and the corresponding Kalman filter based observer in this paper were successfully applied in the real-time Hardware-in-the-loop simulation platform. In addition, compared with literature's model performance in a same HIL simulation platform, the available dSPACE simulation period has been improved to 0.1s from 1s. In addition, the Kalman filter based model shows the ability to simultaneously estimate solid phase surface concentration and SoC, so that it can be applied as the basis for the real-time BMS and relevant battery status monitoring applications, e.g. ageing degradation or fast charging control. In the future, once a commercial battery's parameters are measured accurately, the battery plant will be able to be replaced by the actual battery, and then, this Kalman filter model can be utilized in the vehicle's battery management system for applications.

ACKNOWLEDGMENT

The research presented within this paper is possible thanks to funding provided by Institute of Digital Engineering UK through Virtually Connected Hybrid Vehicle project.

REFERENCES

[1] R. Klein, N. A. Chaturvedi, J. Christensen, J. Ahmed, R. Findeisen, and A. Kojic, "Electrochemical model based observer design for a lithium-ion battery," *IEEE Trans. Control Syst. Technol.*, vol. 21, no. 2, pp. 289–301, 2013.

[2] T. R. Ashwin, A. Barai, K. Uddin, L. Somerville, A. McGordon, and J. Marco, "Prediction of battery storage ageing and solid electrolyte interphase property estimation using an electrochemical model," *J. Power Sources*, vol. 385, pp. 141–147, 2018.

[3] A. P. Schmidt, M. Bitzer, Á. W. Imre, and L. Guzzella, "Experiment-driven electrochemical modeling and systematic parameterization for a lithium-ion battery cell," *J. Power Sources*, vol. 195, no. 15, pp. 5071–5080, Aug. 2010.

[4] X. Han, M. Ouyang, L. Lu, and J. Li, "Simplification of physics-based electrochemical model for lithium ion battery on electric vehicle. Part II: Pseudo-two-dimensional model simplification and state of charge estimation," *J. Power Sources*, vol. 278, pp. 814–825, 2015.

[5] D. Di Domenico, A. Stefanopoulou, and G. Fiengo, "Lithium-Ion Battery State of Charge and Critical Surface Charge Estimation Using an Electrochemical Model-Based Extended Kalman Filter," *J. Dyn. Syst. Meas. Control*, vol. 132, p. 61302, 2010.

[6] S. Santhanagopalan and R. E. White, "Online estimation of the state of charge of a lithium ion cell," *J. Power Source*, vol. 161, pp. 1346–1355, 2006.

[7] S. J. Moura, F. B. Argomedo, R. Klein, A. Mirtabatabaei, and M. Krstic, "Battery state estimation for a single particle model with electrolyte dynamics," *IEEE Trans. Control Syst. Technol.*, vol. 25, no. 2, pp. 453–468, 2017.

[8] X. Han, M. Ouyang, L. Lu, and J. Li, "Simplification of physics-based electrochemical model for lithium ion battery on electric vehicle. Part I: Diffusion simplification and single particle model," *J. Power Sources*, vol. 278, pp. 802–813, 2015.

[9] K. A. Smith, C. D. Rahn, and C.-Y. Wang, "Model Order Reduction of 1D Diffusion Systems Via Residue Grouping," *J. Dyn. Syst. Meas. Control*, vol. 130, no. 1, p. 011012, 2008.

[10] P. A. (Petros A. . Ioannou and J. Sun, *Robust adaptive control*. PTR Prentice-Hall, 1996.

[11] Y. Bar-Shalom, X.-R. Li, and T. Kirubarajan, *Estimation with applications to tracking and navigation*. Wiley, 2001.